

# Scanning Electrochemical Microscopy of Model Neurons: Constant Distance Imaging

Ruwan T. Kurulugama,<sup>†,‡</sup> David O. Wipf,<sup>§</sup> Sara A. Takacs,<sup>||,⊥</sup> Sirinun Pongmayteegul,<sup>||</sup> Paul A. Garriss,<sup>||</sup> and John E. Baur\*,<sup>†</sup>

Departments of Chemistry and Biological Sciences, Illinois State University, Normal, Illinois 61790, and Department of Chemistry, Mississippi State University, Mississippi State, Mississippi 39762

Undifferentiated and differentiated PC12 cells were imaged with the constant-distance mode of scanning electrochemical microscopy (SECM) using carbon ring and carbon fiber tips. Two types of feedback signals were used for distance control: the electrolysis current of a mediator (constant-current mode) and the impedance measured by the SECM tip (constant-impedance mode). The highest resolution was achieved using carbon ring electrodes with the constant-current mode. However, the constant-impedance mode has the important advantages that topography and faradaic current can be measured simultaneously, and because no mediator is required, the imaging can take place directly in the cell growth media. It was found that vesicular release events do not measurably alter the impedance, but the depolarizing solution, 105 mM K<sup>+</sup>, produces a dramatic impedance change such that constant-distance imaging cannot be performed during application of the stimulus. However, by operating the tip in the constant-height mode, cell morphology (via a change in impedance) and vesicular release could be detected simultaneously while moving the tip across the cell. This work represents a significant improvement over previous SECM imaging of model neurons, and it demonstrates that the combination of amperometry and constant-impedance SECM has the potential to be a powerful tool for investigating the spatial distribution of neurotransmitter release *in vitro*.

Since the development of microelectrodes in the 1970s and 1980s, electrochemical methods have played an increasingly prominent role in the field of neuroscience. In fact, the first carbon fiber microelectrodes were developed specifically for the detection of neurotransmitters *in vivo*.<sup>1–3</sup> Carbon microelectrodes have several characteristics, namely, good sensitivity and high temporal

and spatial resolution, that make them well suited for following neurotransmitter dynamics in biological systems.<sup>4–7</sup> One area in which carbon fiber electrodes have seen extensive use is for investigating vesicular release from single cells.<sup>8–11</sup> The technique most commonly employed for such single-cell studies is amperometry, where the potential of a stationary microelectrode is set to a value at which electroactive neurotransmitters are oxidized. Amperometry has the unique ability to detect single vesicular release events in real time, but only release events in proximity to the electrode are detected. In another microelectrode technique, scanning electrochemical microscopy (SECM), a microelectrode is moved systematically across a substrate, thus providing electrochemical or topographical information, or both, about the substrate. The joining of SECM with amperometry should be a powerful tool for studying the spatial distribution of neurotransmitter release during neuronal growth and development. The aim of this work is to demonstrate that SECM is suitable for making high-resolution images of cultured model neurons and to incorporate amperometric techniques into the SECM instrument so that vesicular release and topography can be detected simultaneously with good spatial resolution.

We have previously shown that SECM can be used to image model neurons and detect small changes in cell morphology in real time.<sup>12</sup> However, those results were obtained with the SECM operating in the constant-height mode, where the tip is moved through a constant plane above the substrate throughout the recording. The constant-height mode is disadvantageous for substrates having a high relief, as raised features must be imaged

\* Corresponding author. Fax: (309)438–5538. E-mail: jebaur@ilstu.edu.  
<sup>†</sup> Department of Chemistry, Illinois State University.  
<sup>‡</sup> Current address: Department of Chemistry, Indiana University, Bloomington, IN 47405.  
<sup>§</sup> Department of Chemistry, Mississippi State University.  
<sup>||</sup> Department of Biological Sciences, Illinois State University.  
<sup>⊥</sup> Current address: Department of Neurology, Northwestern University Feinberg School of Medicine, Chicago, IL 60611.

(1) Ponchon, J.-L.; Cespuglio, R.; Gonon, F.; Juvet, M.; Pujol, J.-F. *Anal. Chem.* **1979**, *51*, 1483–1486.  
(2) Dayton, M. A.; Brown, J. C.; Stutts, K. J.; Wightman, R. M. *Anal. Chem.* **1980**, *52*, 946–950.

(3) Gonon, F.; Cespuglio, R.; Ponchon, J.-L.; Buda, M.; Juvet, M.; Adams, R. N.; Pujol, J.-F. *C. R. Hebd. Seances Acad. Sci., Ser. D* **1978**, *286*, 1203–1206.  
(4) Wightman, R. M.; May, L. J.; Michael, A. C. *Anal. Chem.* **1988**, *60*, 769A–779A.  
(5) Hochstetler, S. E.; Puopolo, M.; Gustincich, S.; Raviola, E.; Wightman, R. M. *Anal. Chem.* **2000**, *72*, 489–496.  
(6) Venton, B. J.; Troyer, K. P.; Wightman, R. M. *Anal. Chem.* **2002**, *74*, 539–546.  
(7) Peters, J. L.; Kulagina, N. V.; Yang, H.; Michael, A. C. In *Encyclopedia of Electrochemistry*; Bard, A. J., Stratmann, M., Eds.; Wiley-VCH: Weinheim, Germany, 2002; Vol. 9, pp 463–484.  
(8) Travis, E. R.; Wightman, R. M. *Annu. Rev. Biophys. Biomol. Struct.* **1998**, *27*, 77–103.  
(9) Michael, D. J.; Wightman, R. M. *J. Pharm. Biomed. Anal.* **1999**, *19*, 33–46.  
(10) Chen, G. Y.; Ewing, A. G. *Crit. Rev. Neurobiol.* **1997**, *11*, 59–90.  
(11) Clark, R. A.; Ewing, A. G. *Mol. Neurobiol.* **1997**, *15*, 1–16.  
(12) Liebetrau, J. M.; Miller, H. M.; Baur, J. E.; Takacs, S. A.; Anupunpisit, V.; Garriss, P. A.; Wipf, D. O. *Anal. Chem.* **2003**, *75*, 563–571.

separately from low-lying features to avoid tip–substrate collisions and to ensure that the substrate is within imaging range of the tip. The model neurons used in this work, PC12 cells,<sup>13–15</sup> have extraordinarily high relief by SECM standards. These cells store and release the neurotransmitters dopamine and norepinephrine, and when exposed to nerve growth factor (NGF), they express a neuronal phenotype. The resulting differentiated cells have a cell body proper that is typically 10–20  $\mu\text{m}$  high, while the extending neurites are typically <1–2  $\mu\text{m}$  high and up to tens of micrometers long. Release of the neurotransmitter is readily detectable by amperometry upon chemical stimulation.<sup>16–19</sup>

To image samples of such high relief, it is necessary to operate the SECM in the less common constant-distance mode. This approach requires a distance-dependent signal and feedback circuitry so that the tip can be moved vertically to maintain a constant distance from the substrate. In the simplest implementation, the electrolysis current of a mediator is used as the distance-dependent signal and the tip is moved up or down to maintain a constant current.<sup>20,21</sup> While constant-current imaging is simple and extremely useful for measurements of topography, it requires the mediator to be the sole electroactive species detectable at the tip potential. For biological applications, careful work must be done to ensure that the mediator does not have detrimental physiological effects.

A few techniques have been developed that make use of an alternative distance-dependent signal, the most prominent of which uses shear force feedback.<sup>20,22–32</sup> In this adaptation of a distance control technique from near-field scanning optical microscopy, the SECM tip is driven to its resonant frequency by a piezoelectric oscillator. As the tip approaches a surface, the damping of the tip frequency by the shear force of the solution is detected with a second piezoelectric device or by the deflection of a laser beam. Although this approach is relatively difficult to use with softer,

more pliable substrates, it has recently been demonstrated that line scans of chromaffin and PC12 cells can be recorded using shear force feedback with optical detection and that vesicular release could be detected by the stationary tip.<sup>22,24</sup>

An alternative approach is to use the impedance of the SECM tip as the distance-dependent signal. First used by Bard<sup>33</sup> and further developed by others,<sup>34–37</sup> this technique modulates the impedance signal to a high frequency (typically 10–100 kHz) so that it can be detected separately from the lower frequency voltammetric signals. This approach has three important advantages that make it well-suited for imaging model neurons. First, it requires no mediator, as the ions in solution provide the signal. Second, faradaic current can be detected simultaneously with the detection of morphology. Third, this technique is instrumentally simple compared to the shear-force approach; it requires no electrode modifications and the addition of only a simple electronic circuit.<sup>36</sup>

In this work, we demonstrate that high-resolution topographical images of entire model neurons can be obtained with constant-distance imaging using two types of feedback signals. Micrometer resolution can be achieved with constant-current imaging when using ring electrodes having tip diameters of  $\sim 1\ \mu\text{m}$ .<sup>38</sup> We demonstrate that constant-impedance imaging is feasible at carbon electrodes and that because no exogenous mediator is required, topographic images can be recorded directly in the cell growth media. It is shown that vesicular release does not affect the impedance signal and that morphology (measured by tip impedance) can be detected simultaneously with vesicular release during repetitive line scans. This work represents an important step toward the ultimate goal of functional imaging of neurotransmitter release during neuronal growth and development.

## EXPERIMENTAL SECTION

**Electrodes.** Carbon fiber electrodes were prepared as described previously<sup>39</sup> by sealing carbon fibers with nominal diameters of 5 (Thornel T-650, Cytec, Greenville, SC) or 10  $\mu\text{m}$  (Thornel P-55, Cytec) in pulled glass capillaries. The ratio of the insulator radius to electrode radius for these electrodes was  $\sim 2$ , corresponding to overall tip diameters of 10 and 20  $\mu\text{m}$ , respectively. Carbon ring electrodes with overall tip diameters of <2  $\mu\text{m}$  were prepared as described by Ewing.<sup>38</sup> All electrodes were polished at a 90° angle on a micropipet beveller (Sutter Instrument Co., Novato, CA) with a diamond particle abrasive plate (for the carbon fiber electrodes) or a 0.05- $\mu\text{m}$  alumina particle abrasive plate (for the carbon ring electrodes). Prior to use in the SECM, electrodes were tested using steady-state cyclic voltammetry in 1.0 mM  $\text{Ru}(\text{NH}_3)_6^{3+}$  in phosphate buffer. All data were recorded using a 3 M NaCl Ag/AgCl reference electrode and a Pt wire auxiliary electrode.

- (13) Greene, L. A.; Tischler, A. S. *Proc. Natl. Acad. Sci. U.S.A.* **1976**, *73*, 2424–2428.
- (14) Levi-Montalcini, R. *Science* **1987**, *237*, 1154–1162.
- (15) Batistatou, A.; Greene, L. A. *J. Cell. Biol.* **1991**, *115*, 461–471.
- (16) Zerby, S. E.; Ewing, A. G. *J. Neurochem.* **1996**, *66*, 651–657.
- (17) Zerby, S. E.; Ewing, A. G. *Brain Res.* **1996**, *712*, 1–10.
- (18) Kozminski, K. D.; Gutman, D. A.; Davila, V.; Sulzer, D.; Ewing, A. G. *Anal. Chem.* **1988**, *70*, 3123–3130.
- (19) Chen, T. K.; Luo, G.; Ewing, A. G. *Anal. Chem.* **1994**, *66*, 3031–3035.
- (20) Lee, Y.; Ding, Z.; Bard, A. J. *Anal. Chem.* **2002**, *74*, 3634–3643.
- (21) Wipf, D. O.; Tallman, D. E.; Bard, A. J. *Anal. Chem.* **1993**, *65*, 1373–1377.
- (22) Bauermann, L. P.; Schuhmann, W.; Schulte, A. *Phys. Chem. Chem. Phys.* **2004**, *6*, 4003–4008.
- (23) Hengstenberg, A.; Kranz, C.; Schuhmann, W. *Chem. Eur. J.* **2000**, *6*, 1547–1554.
- (24) Hengstenberg, A.; Blöchl, A.; Dietzel, I. D.; Schuhmann, W. *Angew. Chem., Int. Ed.* **2001**, *40*, 905–908.
- (25) Katemann, B. B.; Schulte, A.; Schuhmann, W. *Chem. Eur. J.* **2003**, *9*, 2025–2033.
- (26) Hirano, Y.; Mase, Y.; Oyamatsu, D.; Yasukawa, T.; Shiku, H.; Matsue, T. *Chem. Sens.* **2004**, *20*, 754–755.
- (27) Etienne, M.; Schulte, A.; Mann, S.; Jordan, G.; Dietzel, I.; Irmgard, D.; Schuhmann, W. *Anal. Chem.* **2004**, *76*, 3682–3688.
- (28) James, P. I.; Garfias-Mesias, L. F.; Moyer, P. J.; Smyrl, W. H. *J. Electrochem. Soc.* **1998**, *145*, L64–L66.
- (29) Smyrl, W. H.; Buchler, M.; Garfias-Mesias, L.; Kerimo, J. *Proc. Electrochem. Soc.* **2000**, *99*–28, 55–65.
- (30) Katemann, B. B.; Schulte, A.; Schuhmann, W. *Electroanal.* **2004**, *16*, 60–65.
- (31) Etienne, M.; Schulte, A.; Schuhmann, W. *Electrochem. Commun.* **2004**, *6*, 288–293.
- (32) Florencia Garay, M.; Ufheil, J.; Borgwarth, K.; Heinze, J. *Phys. Chem. Chem. Phys.* **2004**, *6*, 4028–4033.

- (33) Horrocks, B. R.; Schmidtke, D.; Heller, A.; Bard, A. J. *Anal. Chem.* **1993**, *65*, 3605–3614.
- (34) Katemann, B. B.; Schulte, A.; Calvo, E. J.; Koudelka-Hep, M.; Schuhmann, W. *Electrochem. Commun.* **2002**, *4*, 134–138.
- (35) Katemann, B. B.; Inchauspe, C. G.; Castro, P. A.; Schulte, A.; Calvo, E. J.; Schuhmann, W. *Electrochim. Acta* **2003**, *48*, 1115–1121.
- (36) Alpuche-Aviles, M. A.; Wipf, D. O. *Anal. Chem.* **2001**, *73*, 4873–4881.
- (37) Gabrielli, C.; Huet, F.; Keddam, M.; Rousseau, P.; Vivier, V. *J. Phys. Chem. B* **2004**, *108*, 11620–11626.
- (38) Kim, Y.-T.; Scarnulis, D. M.; Ewing, A. G. *Anal. Chem.* **1986**, *58*, 1782–1786.
- (39) Kelly, R. S.; Wightman, R. M. *Anal. Chim. Acta* **1986**, *187*, 79–87.

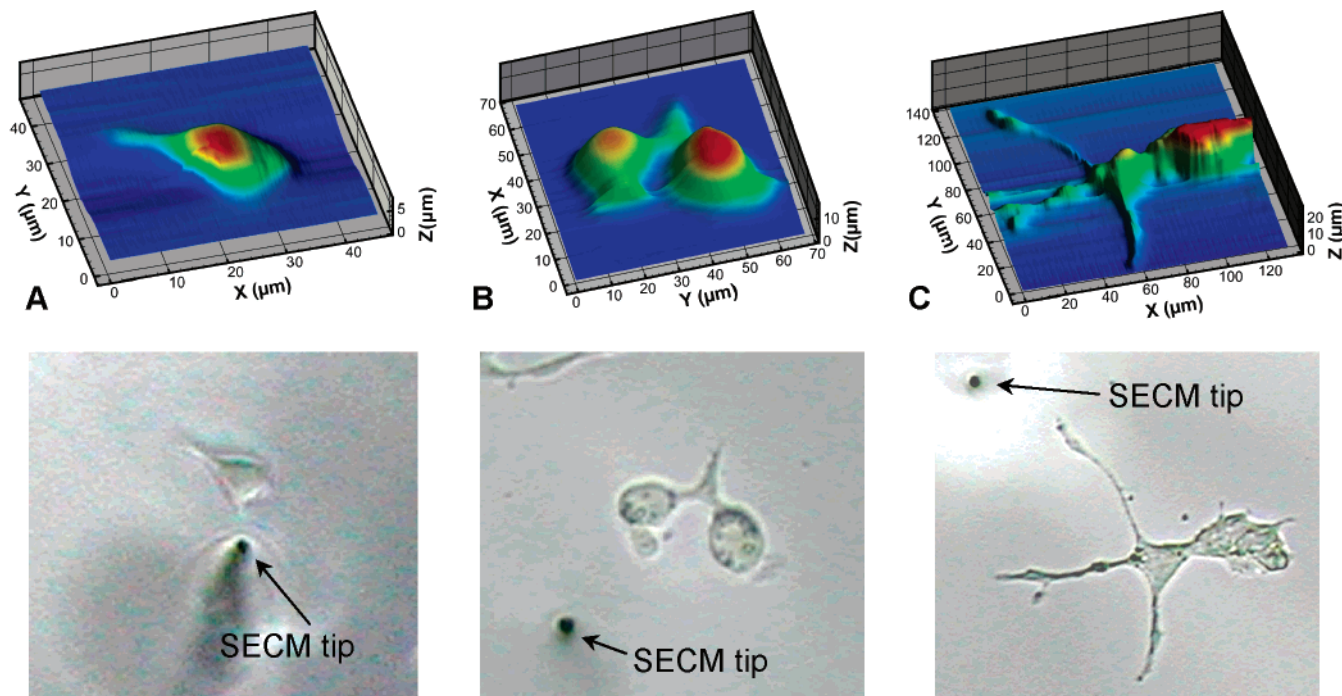


**Figure 1.** Topographic images acquired using constant-current imaging with a  $\sim 1\text{-}\mu\text{m}$ -diameter carbon ring electrode. (A) Undifferentiated PC12 cell; (B) PC12 cells in the early stage of neurite development following exposure to NGF; (C) differentiated PC12 cell. Conditions:  $1.0\text{ mM Ru}(\text{NH}_3)_6^{3+}$  mediator in HBSS,  $E_T = -0.4\text{ V}$ , scan rate  $5\text{ }\mu\text{m/s}$  for (A) and  $6\text{ }\mu\text{m/s}$  for (B) and (C).

**Equipment.** The SECM was identical to that described previously<sup>12,40</sup> with the addition of a feedback circuit,<sup>36,41</sup> a  $z$ -axis piezoelectric pusher with a  $30\text{ }\mu\text{m}$  total travel (Exfo Burleigh, Victor, NY), and a piezo amplifier (Exfo Burleigh) necessary for constant-distance experiments. For constant-current imaging, the feedback circuit moved the tip in the  $z$  direction to the extent necessary to maintain the desired current. This vertical displacement plotted as a function of  $xy$  position produces a topographical image of the substrate. Constant-impedance experiments were conducted using the equipment and circuit described by Alpuche-Aviles and Wipf.<sup>36</sup> A  $90\text{-kHz}$ ,  $10\text{-mV}$  p-p sine wave produced by the lock-in amplifier (Stanford Research Systems, Sunnyvale, CA) was used for impedance measurements. While high frequencies (MHz range) are necessary for the solution resistance to dominate the measured impedance,<sup>36</sup> the lock-in amplifier used for this work had a maximum operating frequency of  $100\text{ kHz}$ . Because of increased noise levels at frequencies close to this limit, however, a value of  $90\text{ kHz}$  was used for all impedance measurements. The output time constant of the lock-in amplifier was between  $1$  and  $30\text{ ms}$ . Tip speeds of  $5\text{--}10\text{ }\mu\text{m/s}$  were used when imaging in the constant-distance mode and up to  $20\text{ }\mu\text{m/s}$  in the constant-height mode. Depolarizing solutions to elicit neurotransmitter release were applied to the cells by pressure ejection with a Picospritzer II (General Valve Corp., Fairfield, NJ) through a micropipet with a tip diameter of  $1\text{--}3\text{ }\mu\text{m}$ . The micropipet was positioned to within  $100\text{ }\mu\text{m}$  of the cell using a hydraulic micromanipulator (Narishige, Tokyo, Japan). All SECM experiments were conducted on the stage of an inverted microscope with phase contrast optics (Olympus America, Melville, NY).

**Cell Culture.** PC12 cells obtained from the American Type Culture Collection (Manassas, VA) were cultured as described previously<sup>12</sup> in RPMI-1640 media (Sigma, St. Louis, MO) supplemented with  $10\%$  horse serum,  $5\%$  fetal bovine serum (Atlanta Biologicals, Norcross, GA),  $100\text{ units mL}^{-1}$  penicillin, and  $100\text{ }\mu\text{g mL}^{-1}$  streptomycin (Sigma). Cultures were incubated at  $37\text{ }^\circ\text{C}$  in a  $5\%$   $\text{CO}_2$  atmosphere, and the growth medium was exchanged every  $2\text{--}3$  days. Cells were subcultured onto new collagen-coated  $50\text{-mL}$  culture flasks (Nalge Nunc, Rochester, NY) every  $7\text{--}10$  days. Isolated single cells were obtained by plating the cells at a density of  $1.8 \times 10^4\text{ cm}^{-2}$  onto  $60 \times 15\text{ mm}$  collagen-coated Petri dishes (Corning, Corning, NY). Release experiments were conducted only near the end of the exponential growth phase ( $6\text{--}8$  days) at isolated individual cells near larger colonies. Differentiated PC12 cells were obtained by plating cells at a density of  $2.2 \times 10^3\text{ cm}^{-2}$  and supplementing the growth media with  $2\text{ nM}$  NGF (Sigma) followed by  $3\text{--}4$  days of incubation.

**Solutions.** For constant-current imaging, the mediator was  $1.0\text{ mM Ru}(\text{NH}_3)_6^{3+}$  in pH  $7.4$  Hank's balanced salt solution (HBSS, Sigma) with  $10\text{ mM}$  HEPES. Constant-impedance imaging was carried out either in HBSS with  $10\text{ mM}$  HEPES (but without mediator) or directly in the supplemented RPMI-1640 growth media (also without mediator). For release experiments, a depolarizing solution was prepared in which the  $\text{Na}^+$  in the HBSS was replaced with a  $\text{K}^+$  on a  $1:1$  molar basis so that the final concentration of  $\text{K}^+$  was  $105\text{ mM}$ . All solutions were prepared in  $18\text{ M}\Omega\cdot\text{cm}$  deionized water (NanoPure system, Barnstead-Thermolyne, Inc., Dubuque, IA).

## RESULTS AND DISCUSSION

**Constant-Current Imaging.** Figure 1 shows representative topographical images of undifferentiated (i.e., no NGF treatment)

(40) Spaine, T. W.; Baur, J. E. *Anal. Chem.* **2001**, *73*, 930–938.

(41) Wipf, D. O. In *Scanning Electrochemical Microscopy*; Bard, A. J., Mirkin, M. V., Eds.; Marcel Dekker: New York, 2001; pp 17–74.



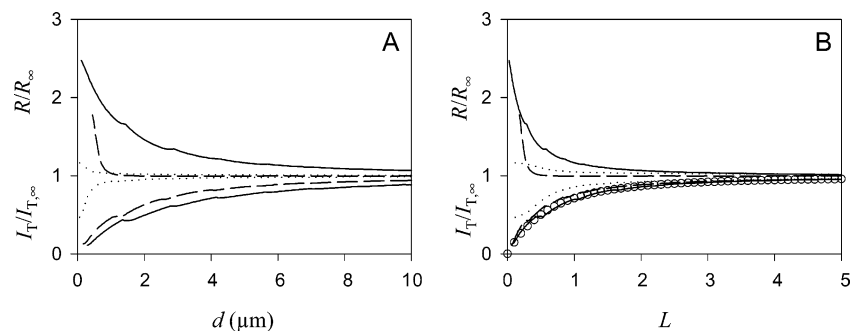


**Figure 2.** Normalized current ( $I/I_\infty$ ) and normalized impedance ( $R/R_\infty$ ) approach curves recorded with a 10- $\mu\text{m}$ -diameter carbon fiber electrode (solid line), a 5- $\mu\text{m}$ -diameter carbon fiber electrode (dashed line), and a  $\sim 1\text{-}\mu\text{m}$ -diameter carbon ring electrode (dotted line). Approach curves are plotted as a function of (A)  $d$ , the tip–substrate separation (in  $\mu\text{m}$ ) and (B)  $L$ , the tip–substrate separation normalized by the nominal electrode radius,  $a$  (disk electrodes), or by the outer radius of the ring electrode,  $b$ . In both panels, the upper curves correspond to the impedance measurements and the lower curves correspond to the current measurements. The open circles represent the theoretical response for a disk electrode with  $\text{RG} = 2.03$ .<sup>45</sup> Conditions: 1.0 mM  $\text{Ru}(\text{NH}_3)_6^{3+}$  in Hank's buffer,  $E_T = -0.4$  V, substrate, uncoated plastic Petri dish.

and differentiated (NGF-treated) PC12 cells recorded with carbon ring electrodes ( $\sim 1\text{-}\mu\text{m}$  diameter) using the constant-current imaging mode. Each corresponding optical micrograph shows the imaged cell and the electrode used to record the image. These data were collected in HBSS using  $\text{Ru}(\text{NH}_3)_6^{3+}$  as the mediator. In contrast to previous images of PC12 cells recorded in the constant-height mode,<sup>12</sup> the constant-current mode is clearly capable of providing detailed topographical images of the entire cell. The SECM image of Figure 1A shows the elongation of an undifferentiated PC12 cell and a short process emitted by the cell. In Figure 1B, the processes of two closely spaced cells have formed a connection that is reproduced by the SECM topographical image. Figure 1C shows a wider-field image of a typical differentiated PC12 cell. Although most regions of the differentiated cell's morphology are accurately obtained, it is apparent that there are some regions where tip–substrate collisions have occurred (e.g., near  $x, y = 5, 70$ ), resulting in streaked images. Near the cell body proper (approximately  $x, y = 120, 60$ ) the height of the cell is large enough that the vertical limit of the piezopusher is reached. The resulting tip–substrate collision likely accounts for some of the streaking evident in the image line scans between  $y = 60$  and  $y = 80$ . The frequency of these types of artifacts can be reduced by careful selection of the zero point of the  $z$ -axis piezopusher (just below the lowest point of the substrate), but the large areas over which the tip must be rastered in order to image an entire differentiated cell increases the likelihood of encountering regions of high topography that can produce such artifacts.

Figure 1 clearly demonstrates that high-resolution images of the entire cell can be obtained with constant-current imaging at carbon ring electrodes. In cases where detection of cell morphology alone is needed, constant-current imaging is useful because it is instrumentally simple, and it can be used with very small electrodes. However, there are two important limitations of this technique that preclude its use for imaging both morphology and function. First, a moderate concentration (typically 1 mM) of an exogenous mediator is required to provide the feedback signal. Although an endogenous species such as  $\text{O}_2$  could be used, variations in the concentrations of such endogenous compounds can also have a biological origin<sup>42–44</sup> and thus are not suitable for use as a feedback signal. Efforts have been made to select biocompatible mediators for SECM of living cells,<sup>12</sup> but in the

presence of a relatively high concentration of an exogenous species, especially one with facile redox characteristics, there always exist possible unwanted interactions between the mediator and the cells or between the mediator and released species. The second limitation is that any electroactive species released by the cell that is also detectable at the tip potential will affect the accuracy of the topographical image. It is conceivable to record sequential topographical (using the constant-current mode) and chemical images (by retracing a stored topography), but this would require extra time and a means to flush the mediator solution from the culture dish. The constant-impedance mode promises to avoid these complications, so further effort was directed toward that approach.

**Constant-Impedance Imaging.** Simultaneous impedance and amperometric approach curves were recorded at two different sizes of carbon fiber disk electrodes and at a  $\sim 1\text{-}\mu\text{m}$ -diameter carbon ring electrode in order to characterize the distance dependence of the tip impedance (Figure 2). These curves were recorded for the approach to an insulating, planar substrate (the bottom of the Petri dish before collagen coating). The current approach curves for the two disk electrodes fit theory for negative feedback with electrodes having  $\text{RG} = 2.03$ <sup>45</sup> as shown by the normalized approach curves in Figure 2B. The current approach curve for the ring electrode has a steeper distance dependence than the disk electrodes, consistent with previous results for SECM with ring electrodes.<sup>46</sup> Of more interest is the behavior of the impedance approach curves, which is more complex. As expected,<sup>36</sup> the impedance for all three types of electrodes is observed to increase as the tip–substrate distance is reduced. However, the approach curve for the ring electrode indicates that it may be poorly suited to constant-impedance imaging. The magnitude of its change is the smallest of the three electrodes, and the working range is only from about  $L = 0.8$ , where the impedance starts to deviate from  $R_\infty$ , to about  $L = 0.3$ , where the tip contacts the substrate. This short working distance (0.15–0.40  $\mu\text{m}$ ) and the relatively low signal-to-noise ratio of the impedance signal (compared to the carbon fiber electrodes) have

(42) Takii, Y.; Takoh, K.; Nishizawa, M.; Matsue, T. *Electrochim. Acta* **2003**, *48*, 3381–3385.

(43) Yasukawa, T.; Kaya, T.; Matsue, T. *Chem. Lett.* **1999**, 975–976.

(44) Yasukawa, T.; Kaya, T.; Matsue, T. *Anal. Chem.* **1999**, *71*, 4637–4641.

(45) Amphlett, J. L.; Denuault, G. *J. Phys. Chem. B* **1998**, *102*, 9946–9951.

(46) Lee, Y.; Amemiya, S.; Bard, A. J. *Anal. Chem.* **2001**, *73*, 2261–2267.

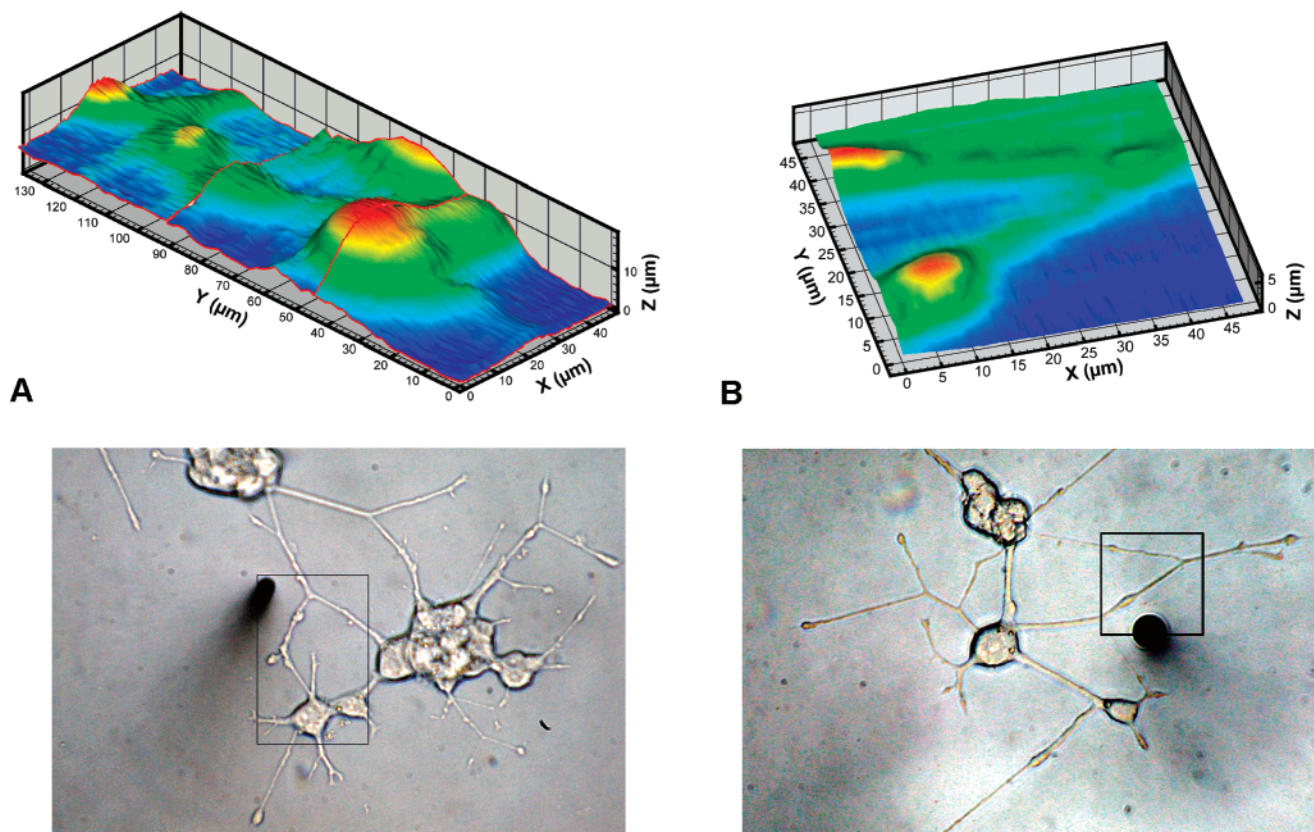


**Figure 3.** Topographic images of differentiated PC12 cells acquired using constant-impedance imaging. (A) Mosaic image of several cells joined by neurites recorded in supplemented RPMI 1640 growth media; (B) closeup image of a neurite bifurcation recorded in HBSS. Conditions: 5- $\mu\text{m}$ -diameter carbon fiber electrode,  $E_T = +0.75\text{ V}$ , no mediator, and scan rate 7  $\mu\text{m/s}$ .

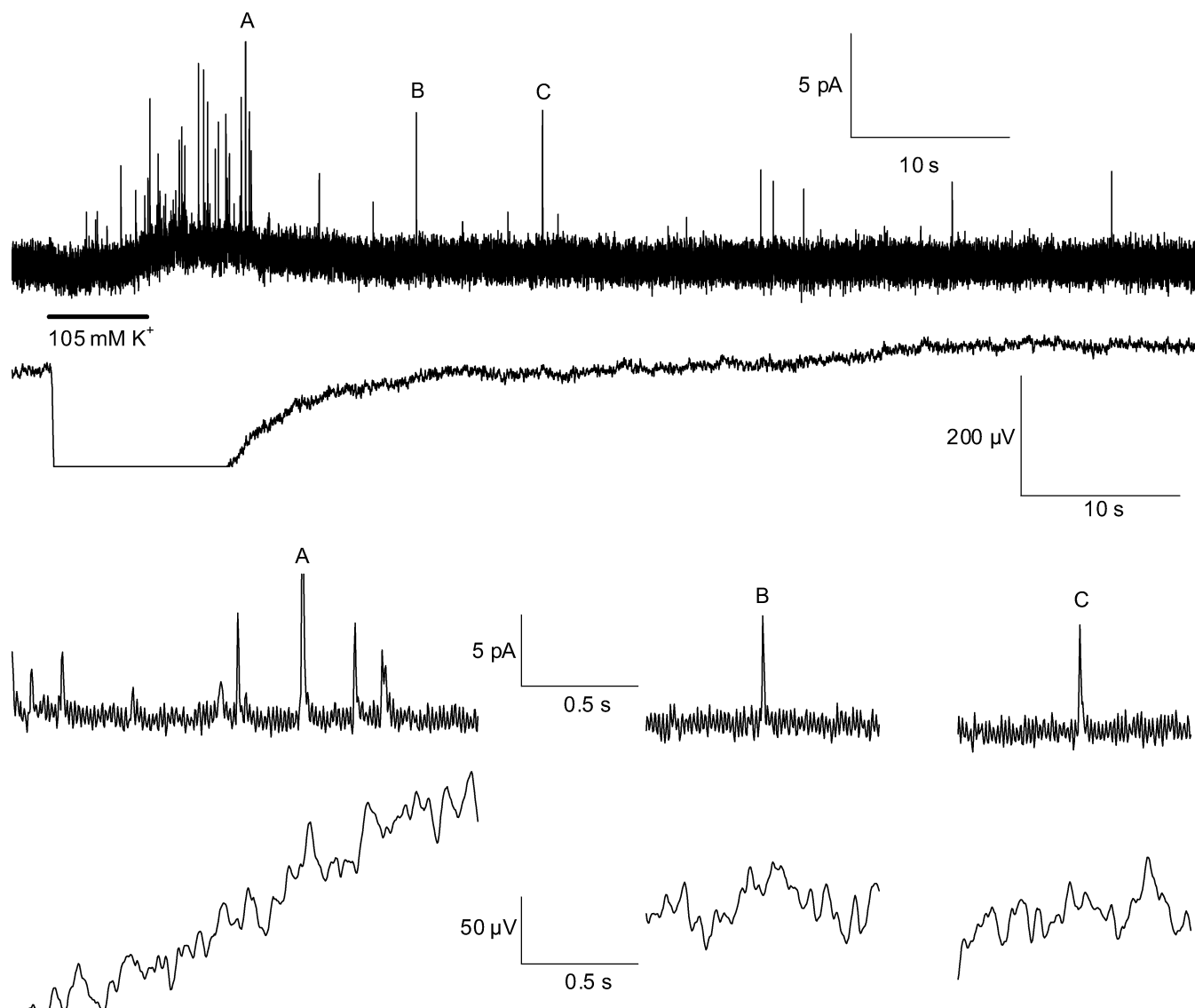
so far precluded the use of the smaller ring electrodes for routine imaging with the impedance mode. Instead, the carbon fiber electrodes were used for constant-impedance imaging. Although the 10- $\mu\text{m}$ -diameter carbon fiber electrodes have a satisfactory tip-substrate dependence of the impedance, their relatively large size prevents the acquisition of highly detailed topographical images. The 5- $\mu\text{m}$ -diameter carbon fiber electrodes represent a midpoint between the ring electrodes and the 10- $\mu\text{m}$ -diameter carbon fiber electrodes (in terms of both tip size and impedance signal-to-noise ratio) and were therefore used for all subsequent constant-impedance imaging of the model neurons.

Figure 3 shows constant-impedance images of differentiated PC12 cells. Figure 3A is a mosaic of three images that shows all or parts of three cell body proper connected by neurites. Varicosities are clearly visible at different regions on these neurites. Importantly, this image was recorded directly in the cell culture medium. The image is somewhat noisy because the time constant of the lock-in amplifier was reduced in order to improve the temporal response of the feedback circuit. This was often necessary when imaging regions with high relief. Figure 3B is a closeup view of a branching neurite that shows two distinct varicosities. Note that the relief of this region is much lower; the  $z$  scale of this image is one-third that of Figure 3A. Clearly the topography of even the low-lying neurites can be imaged using the constant-impedance mode. Additionally, the fact that images can be recorded in the growth media without added mediator opens the possibility of long-term imaging during growth and development.

The resolution of the constant-impedance images of Figure 3 is clearly better than those that can be obtained with constant-height imaging.<sup>12</sup> However, because the 5- $\mu\text{m}$ -diameter carbon fiber electrode must be held relatively far from the substrate to prevent the glass insulator from contacting the substrate (best results were obtained with the tip at approximately 80–95% of  $R_{\infty}$ ), the resolution does not approach that obtained with constant-current imaging (Figure 1).

**Simultaneous Measurement of Impedance and Neurotransmitter Release.** The catecholamine secretory vesicles in PC12 cells contain an ionic environment significantly different from the extracellular media. The water content of these vesicles is only 62%, and they contain high concentrations of dopamine, ATP, and protein.<sup>47</sup> Thus, a potential drawback of using constant-impedance imaging is that during vesicular release the local impedance will change enough so that constant-distance conditions cannot be maintained. To address this concern, release experiments were conducted with a stationary tip so that the impedance signal could be monitored for any changes occurring simultaneously with vesicular release. Figure 4 shows the data for a typical release experiment using 105 mM  $\text{K}^+$  to depolarize the cell membrane and evoke vesicular release. It is immediately apparent that the application of the  $\text{K}^+$  solution causes a large decrease in the measured impedance (i.e., an increase in conductivity). Although this impedance recovers to baseline levels within seconds after the end of the stimulus, this large change

(47) Wagner, J. A. *J. Neurochem.* **1985**, *45*, 1244–1253.



**Figure 4.** Simultaneous recordings of the current (upper trace) and tip impedance (lower trace) recorded with a stationary tip during a 6-s  $K^+$  stimulus at an undifferentiated PC12 cell. Expanded views of the release events having the largest current are shown in (A–C). Conditions: HBSS (no mediator), 5- $\mu$ m-diameter carbon fiber electrode,  $E_T = +0.75$  V, and lock-in amplifier time constant, 1 ms.

makes it impossible to investigate the dependence of the impedance signal on vesicular release during the most active period of release. However, it is possible to investigate more isolated release events occurring after the impedance returns on-scale (Figure 4A–C). Significantly, the expanded regions at the lower portion of Figure 4 show no changes in the impedance above the noise level corresponding to the release events. The absence of such a correlation indicates that the constant-impedance mode is in fact suitable for maintaining distance control during vesicular release, at least during isolated release events. It should be noted that the signal-to-noise ratio of the impedance signal in Figure 4A is low because these data were recorded with a minimal time constant. This was necessary to avoid overfiltering of any transient changes in the impedance occurring simultaneously with release.

The large change in background impedance following application of the 105 mM  $K^+$  solution is potentially much more problematic, as under constant-impedance control, the circuit compensates for the decrease in impedance by moving the tip toward the cell. Unfortunately, the magnitude and speed of the

impedance change causes a sudden and dramatic movement of the tip to the lower travel limit of the z-axis piezopusher, resulting in at best an impaled cell and at worst a shattered tip. It is thus clear that during depolarization with a 105 mM  $K^+$  solution constant-impedance distance control is not possible.

Despite this drawback, it is still possible to use the impedance signal to record simultaneous topographical and chemical information by using the constant-distance mode instead. Figure 5 shows the tip current and tip impedance recorded during repetitive line scans above an undifferentiated PC12 cell concomitant with the application of 105 mM  $K^+$ . For this experiment, the tip was positioned 1–2  $\mu$ m from the apex of the cell and line scans in the  $x$  dimension were recorded at a constant  $y$  position. Here the amperometric signal records the vesicular release of neurotransmitter while the impedance signal is a measurement of tip–substrate separation, or substrate height. The change in background impedance with the application of the high- $K^+$  solution is noticeable but does not obscure the variations in impedance arising from the cell morphology. The release events are clearly

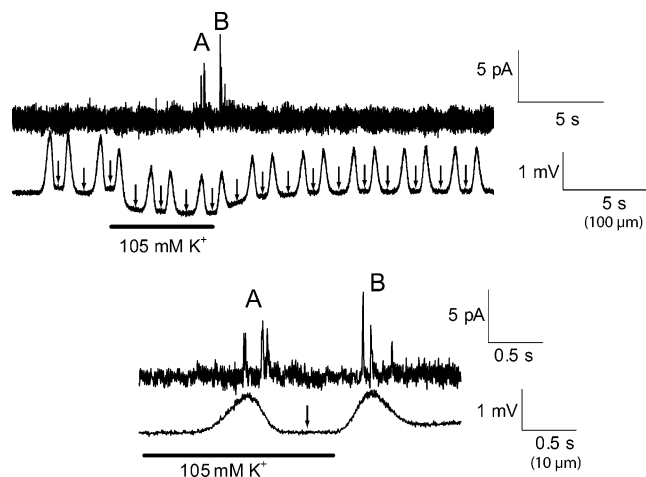


**Figure 5.** Simultaneous recordings of release by amperometry (upper trace) and cell morphology by tip impedance (lower trace) during a 6-s  $K^+$  stimulus at an undifferentiated PC12 cell. The data were recorded during repeated line scans in the  $x$  direction at a constant  $y$  location. To maximize the number of release events detected, relatively high scan rates were used so that multiple passes could be made during and just after application of the stimulus solution. Arrows denote changes in direction (i.e., forward/reverse) of the  $x$  line scan. Conditions: HBSS (no mediator), 5- $\mu$ m-diameter carbon fiber electrode,  $E_T = +0.75$  V, and scan rate 20  $\mu$ m/s.

in phase with the impedance signal, indicating that release is only detected when the tip is over the cell. Fewer release events are recorded because the tip spends only a relatively small fraction of time over the cell. Additionally, it is known that the relative locations of the release sites on the cell and the tip can affect the size and shape of the observed current,<sup>48</sup> and thus, the movement of the tip further complicates the response. The inset of Figure 5 shows an expanded view of the two signals. For each pass over the cell, three release events were detected during the  $\sim 0.5$  s that the tip was over the cell. The absence of detected release after termination of the stimulus is not unexpected, as there is a low probability that the sporadic release events occurring long after the application of the depolarization solution (see, for example, Figure 4) will occur while the electrode is over the release site. Additionally, the vertical position of the electrode was

set high enough to prevent tip–substrate collisions during the line scans (1–2  $\mu$ m). This fact, combined with the curvature of the cell, means that only release sites at the apex of the cell (where the tip–substrate distance is at its minimum) are detected.

## CONCLUSIONS

This work demonstrates that, when operated in the constant-distance mode, the SECM can be used to acquire high-resolution images of model neurons. The highest resolution in this work was achieved using  $\sim 1$ - $\mu$ m carbon ring tips and the electrolysis current of an exogenous redox mediator as the distance control signal. We have also demonstrated that the tip impedance-based constant-distance mode can be used to image the morphology of the model neurons directly in the cell growth media without a redox mediator. This means that long-term studies of neuronal development, degeneration, or both are eminently feasible. It was also demonstrated that neurotransmitter release and morphology can be detected simultaneously using constant-height imaging. These results demonstrate the power and potential of the SECM for spatially mapping the locations of release sites during neuronal growth and development.

Clearly, for spatial mapping of release sites in real time, constant-distance control is essential. Therefore, strategies for achieving constant-distance control during the application of the stimulus include matching the depolarizing solution impedance with the extracellular media and by using alternate secretagogues. Efforts are also being directed toward identifying suitable conditions so that the constant-impedance mode can be used at carbon ring electrodes, which is necessary for simultaneous, high-resolution topographical and chemical imaging of the model neurons.

## ACKNOWLEDGMENT

This work was supported by a grant from the National Science Foundation (DBI-9987028). We are grateful to Kim Garriss for assistance with the cell culture.

Received for review September 25, 2004. Accepted November 17, 2004.

AC048571N

(48) Fan, T.-H.; Fedorov, A. G. *Anal. Chem.* **2004**, *76*, 4395–4405.